



Analysis of Binary Hybrid Nanocomposite Sensor for Acetone Detection at Room Temperature

*Nurul Athirah Abu Hussein, Huzein Fahmi Hawari **

Department of Electrical & Electronic Engineering, Universiti Teknologi PETRONAS, 32610, Seri Iskandar, Perak, Malaysia.

Abstract

Detection of VOCs has been a great important in various fields including environmental monitoring, occupational safety, product quality, and indoor air quality. It can help to identify the sources of pollution, assess health risk, and ensure regulatory compliance. The current study aimed to determine the optimal concentration ratio of binary hybrid material Fe₃O₄-RGO for VOC sensing at room temperature. The materials were synthesized using in-situ method where the concentration of Fe₃O₄ and RGO is varied. The samples prepared were 5, 10, 20, 30, and 40wt% Fe₃O₄-RGO. FTIR analysis showed all functional groups of the single constituents' material exist within the binary hybrid nanocomposite material. SEM analysis shows that the Fe₃O₄ nanoparticles were fully encapsulated in the RGO sheet. The samples were then investigated for their sensing performance in terms of response and recovery time. From the results, it was shown that sample with 10wt% Fe₃O₄-RGO has better performance compared to the rest of the samples.

Keywords: Binary hybrid nanoparticle, Acetone sensing, Room temperature

Full length article *Corresponding Author, e-mail: huzeinmahmi.hawari@utp.edu.my

1. Introduction

Volatile organic compounds (VOCs) are organic chemicals with high vapor pressure at room temperature. They are emitted from various sources including industrial processes, building materials, consumer products, and transportation [1-2]. Some VOCs have been identified as air pollutants that have harmful effects on human health and the environment. Exposure to VOCs can lead to a variety of health effects, including eye, nose, and throat irritation, headaches, dizziness, and nausea [3]. Some VOCs, such as benzene and formaldehyde, are known or suspected carcinogens that can increase the risk of cancer following long-term exposure [4-6]. It is important to identify and eliminate sources of pollution to reduce the levels of VOCs in indoor air. This can be achieved by using natural cleaning products, properly ventilating the building, and choosing low-VOC products when possible. Air purifiers and plants can also help remove VOCs from the air. In addition, the use of an ideal sensor is essential. An ideal sensor is a sensor that can accurately and reliably measure the physical, chemical, or biological properties of interest without interfering with the system being measured. The characteristics of an ideal sensor include high sensitivity, high selectivity, high accuracy, high stability, fast response and recovery times, low cost and ease of use [7].

Although it may not be possible to create a sensor that meets all these characteristics perfectly, designing sensors that are as close as possible to these ideal specifications is an important goal in sensor development. Conventional MOX sensors are the most promising for the monitoring of hazardous VOCs. They are in great demand in a wide range of industries because of their multiple advantages, including powerful response, compact dimensions, ease of use, quick reaction, consistent repeatability for reuse in the same process, simplicity of manufacturing, low detection limits, low energy consumption, and low cost [8]. Although MOX sensors have many advantages, there are also some drawbacks to their use. Some of these drawbacks include low sensitivity to humidity, limited selectivity, and short lifespan owing to the high operating temperature. Despite these drawbacks, MOX sensors are still widely used for detecting VOCs in a variety of applications, and ongoing research has focused on improving their performance and addressing some of these limitations [9]. One of the ongoing methods for improving the performance of MOX sensors is to tailor the active material used in the sensor [10-11]. The active material in a sensor directly interacts with the target analyte or the substance being detected. In the case of gas sensors, the active material is typically a thin film or layer of material that interacts with gas molecules to produce a measurable signal or response.

For example, in a conventional MOX sensor, the active material is a metal oxide such as tin oxide or tungsten oxide. When a metal oxide is exposed to a target gas, gas molecules are adsorbed onto the surface of the metal oxide, which changes its electrical conductivity. The change in conductivity was then measured and used to determine the concentration of the target gas. The properties of the active material are critical to the performance of sensors, and researchers are constantly working to develop new and improved active materials that can increase the sensitivity, selectivity, and accuracy of sensors. Therefore, in this work, we functionalized a metal oxide nanomaterial with reduced graphene oxide to tune the large energy gap in graphene via the quantum confinement effect. The synergistic effect of these two binary hybrid materials is expected to improve the sensor performance.

2. Materials and Methods

2.1. Materials

Iron (II) Chloride Tetrahydrate ($\text{FeCl}_2 \cdot 4\text{H}_2\text{O}$), Iron (III) Chloride Hexahydrate ($\text{FeCl}_3 \cdot 6\text{H}_2\text{O}$), Iron (III) Nitrate ($\text{Fe}(\text{NO}_3)_3 \cdot 9\text{H}_2\text{O}$), Ammonium hydroxide (25%), Nitric acid (65%), Hydrochloric acid (37%), Ascorbic Acid and Graphene oxide (GO) paste (95 wt% purity) were all purchased from Merck. De-ionized (DI) water is used in all preparations. IDE with size of 5mm x 5mm was purchased from NovaScientific.

2.2. Synthesis of Iron oxide (Fe_3O_4)

Fe_3O_4 was synthesized using Massart's procedure as mentioned in by mixing FeCl_2 and FeCl_3 together [12]. The solution of ammonium hydroxide was added to the mixture. The precipitate of black magnetite (Fe_3O_4) was created in an instant. The solution was rinsed several times with DI water before being treated with nitric acid. Lastly, the solution was mixed with ferric nitrate solution to produce the final product.

2.3. Synthesis of RGO

RGO was created in accordance with earlier research [13-14] where 15ml of GO paste was mixed in 50ml of distilled water. The sample was sonicated for about 20 minutes to agitate the mixture to break up the particles for the reducing process. 0.1g of ascorbic acid was then added to the mixture. Next, the sample was heated up to 90°C for 2 hours, filtered, and washed with distilled water.

2.4. Synthesis of the hybrid material

The binary hybrid material was prepared using in-situ method same as the RGO process but 5, 10, 20, 30 and 40wt% of Iron Oxide were first dissolved in GO paste for 30 minutes.

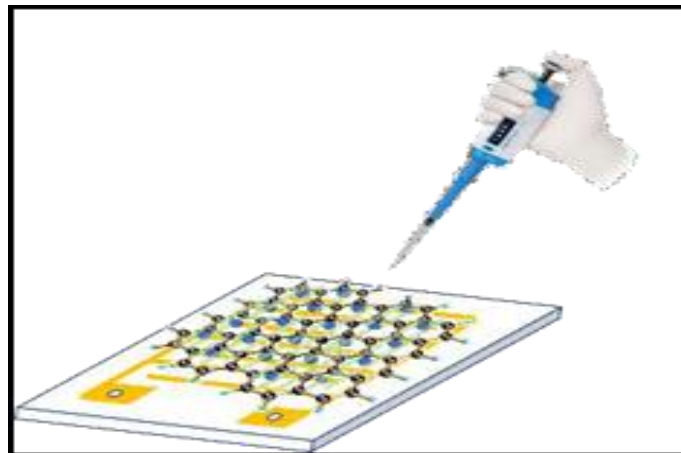


Fig. 1. Deposition of samples on IDE

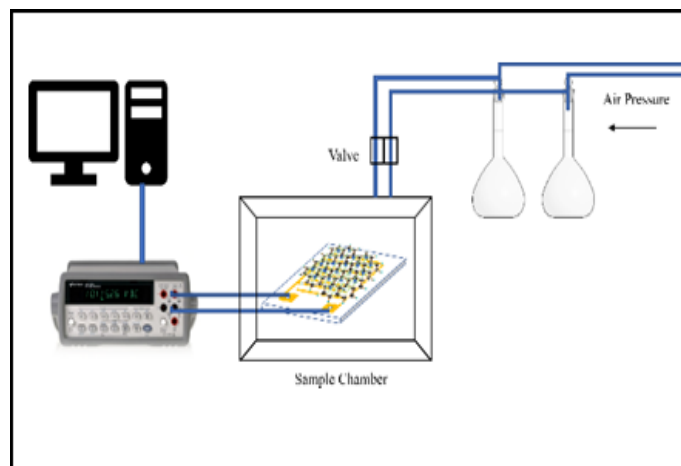


Fig. 2. Gas sensing setup

2.5. Deposition of samples on IDE

0.5 μ l of the as-synthesized materials were deposited on 5mm x 5mm IDE as illustrated in **Fig. 1**. The sample was put on a chamber and gas sensing setup is illustrated in **Fig. 2**.

3. Results and discussion

3.1. FTIR analysis

FTIR analysis is a spectroscopic technique used to identify and analyze the chemical composition of a sample. This involves measuring the interaction of the sample with infrared radiation, which can provide information about the functional groups and chemical bonds present in the sample. **Fig. 3** shows the FTIR spectra of Fe₃O₄, RGO, and 10wt% Fe₃O₄-RGO. Spectra were recorded from 4000 to 4000 cm⁻¹.

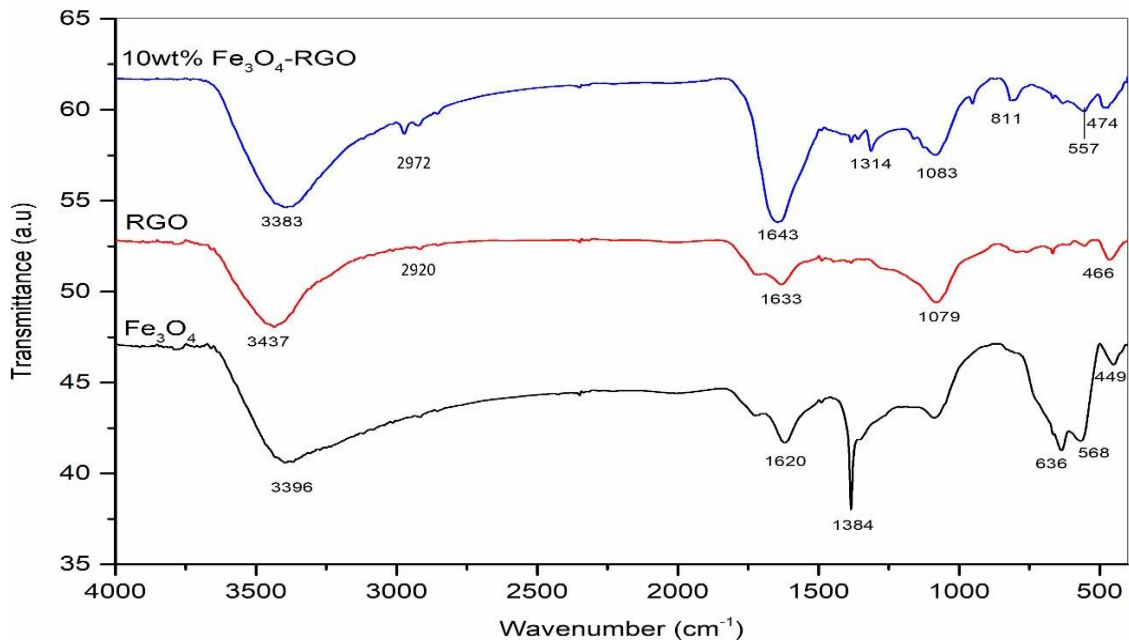


Fig. 3. FTIR Analysis of the single constituents and the binary hybrid material

The spectrum of the binary hybrid material was similar to that of Fe₃O₄ and RGO. This suggests a link between these materials. The minor position change might have been caused by the physical contact between the remaining oxygenated groups in magnetite or RGO.

3.2. Surface and morphological analysis

Further studies were performed on the surface morphology of the samples using scanning electron microscopy (SEM). The as-synthesized Fe₃O₄ nanoparticles, RGO, and 10wt% Fe₃O₄-RGO nanocomposite were dried, and the powders were deposited on a carbon strip. The secondary electron beam had an energy up to 25 keV. **Fig. 4 (a)** shows a clear, wrinkled surface of RGO at a magnification of 5 μ m. The EDX analysis in Figure 5(a) clearly showed the presence of carbon and oxygen at weight percentages of 65.29% and 34.71%, respectively. **Fig. 4 (b)** shows an image of rough and aggregated crystalline Fe₃O₄ nanoparticles, which is due to their natural tendency to aggregate because of their magnetic characteristics.

Abu Hussein et al., 2023

The Fe₃O₄ spectrum shows three characteristic peaks of the stretching Fe-O band at 449, 568, and 636 cm⁻¹. The peaks at 1088 and 1384 cm⁻¹ identified the stretching and bending vibrations of C-O and H-O-H, respectively. The peak at 1621 cm⁻¹ was due to the bending vibration of the absorbed water and surface hydroxyl groups. The last peak at 3396 cm⁻¹ is the stretching of the O-H group. The results are in accordance with the previous research done by [15]. The FTIR results showed that the as-synthesized nanoparticles were Fe₃O₄, without any impurities. In the FTIR spectrum of RGO shown in **Fig. 3**, the peak at 3437 cm⁻¹ is correlated with the hydroxyl group (O-H), whereas the peaks at 2920 cm⁻¹ and 1633 cm⁻¹ correspond to the stretching of the alkane (C-H) and alkene (C = C) groups, respectively. The peak at 1079 cm⁻¹ is ascribed to the stretching vibration of the alcohol group (C-O) [16].

Fig. 4 (c) shows a folding-like image of the surface of the sample. This indicates that the iron oxide nanoparticles were successfully encapsulated in the RGO sheet. The EDX analysis in **Fig. 5 (b)** also shows the presence of Fe, C, and O at 49.41, 23.43%, and 27.16%, respectively. The morphological for both Fe₃O₄ and RGO is in accordance with the description from [17].

3.3. Gas sensing analysis

The sensor responses of the single-material Fe₃O₄ are discussed in while the RGO and hybrid nanoparticles containing 10wt% of Fe₃O₄-RGO are shown in **Fig. 6** upon exposure to 100ppm acetone at room temperature [18]. The response time is defined as the time from the first contact of the sensor with acetone vapor which the sensor resistance reached 90% of the saturated value of the resistance in acetone vapor which is within both red lines in **Fig. 6**. The recovery time is the time from when the acetone resistance returns to 10% from the baseline which is within the blue lines in **Fig. 6**.

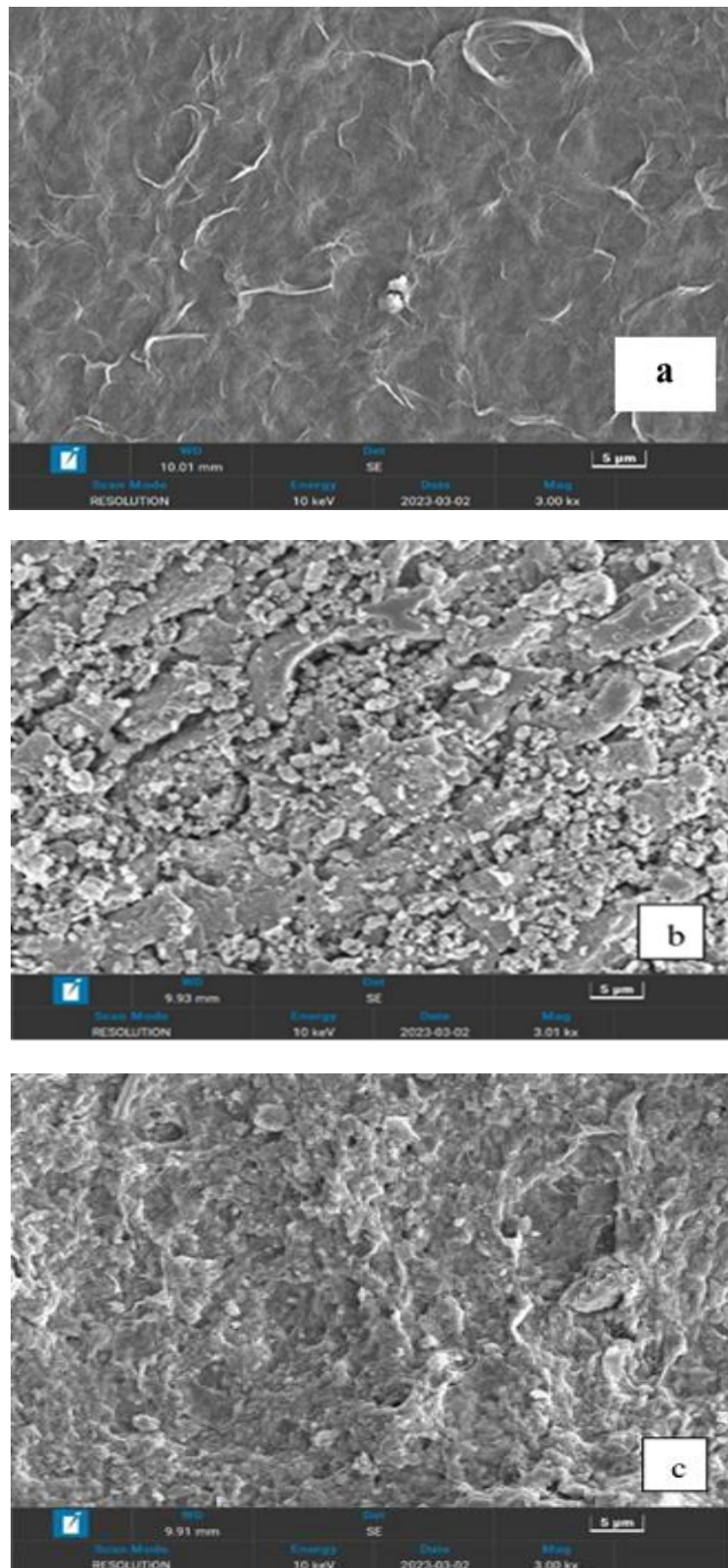


Fig. 4. SEM analysis of (a) RGO (b) Fe₃O₄ and (c) 10wt% Fe₃O₄-RGO

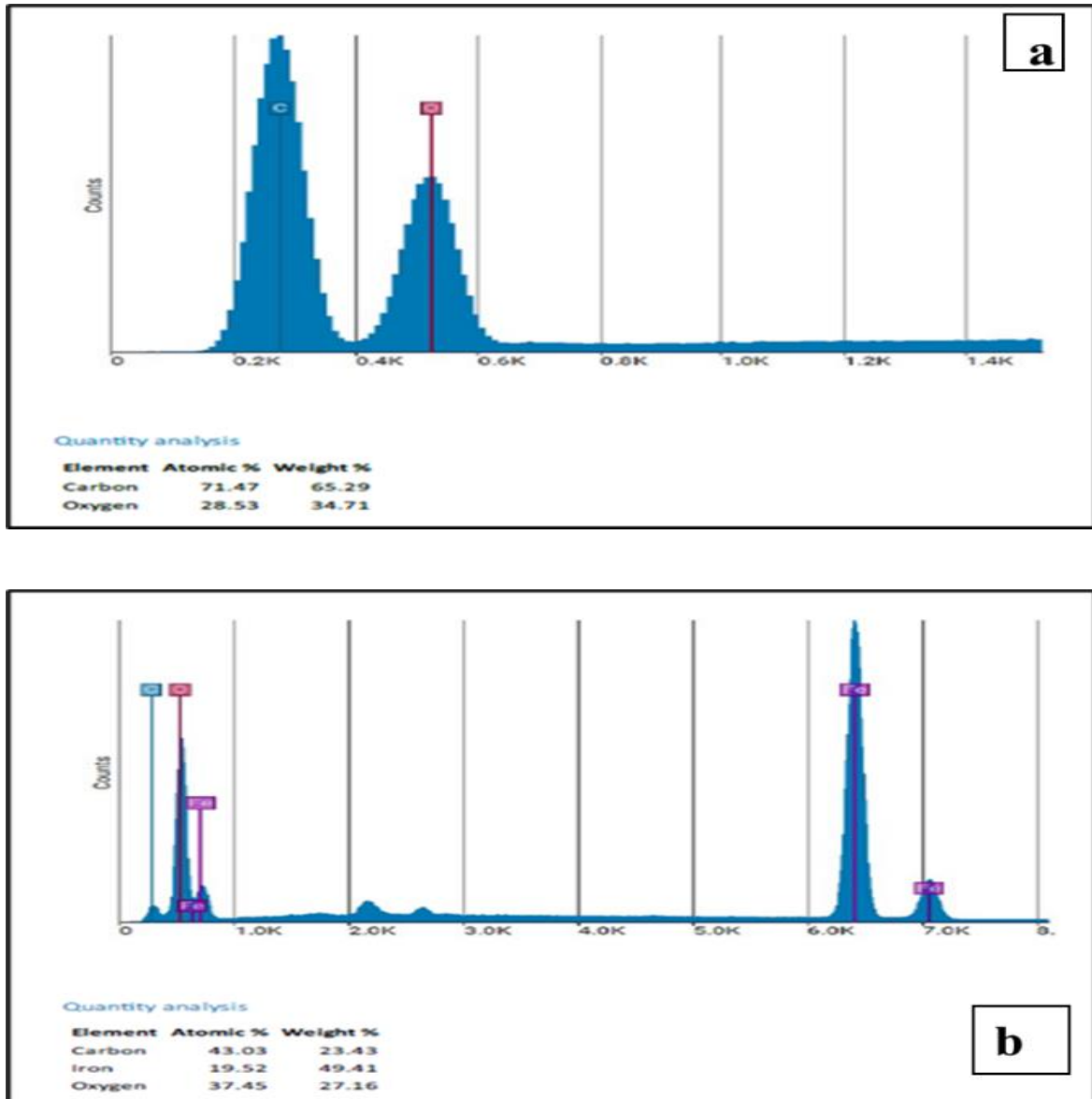


Fig. 5. EDX composition of (a) RGO and (b) 10wt% Fe₃O₄-RGO

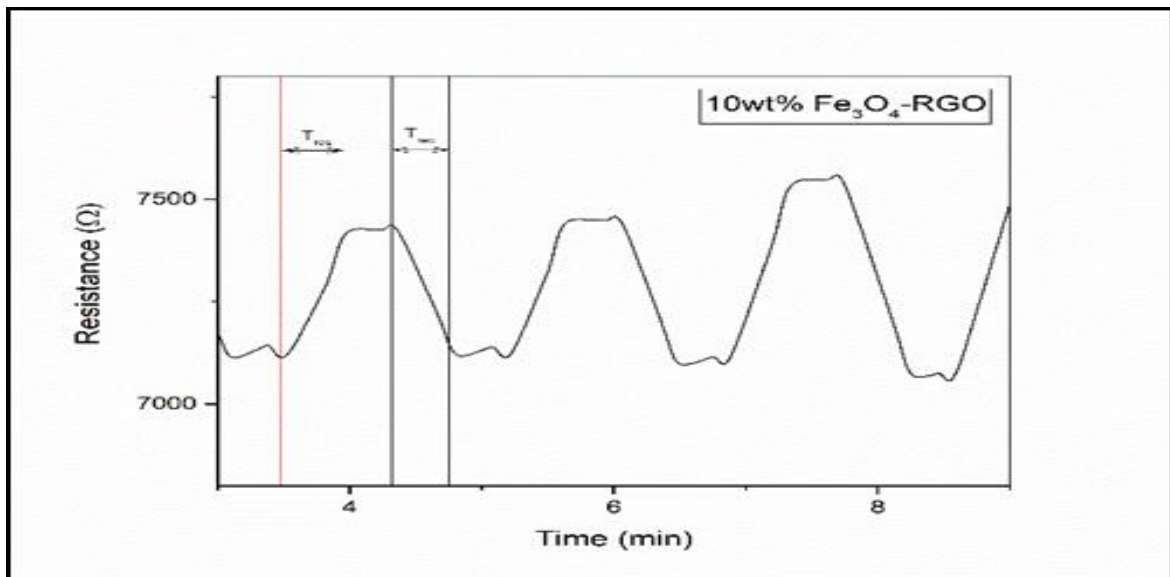


Fig.6. Sensing graph for sample (a) RGO (b) 5wt%, (c) 10wt%, (d) 20wt%, (e) 30wt%, and (f) 40wt% Fe₃O₄-RGO
 Abu Hussein et al., 2023

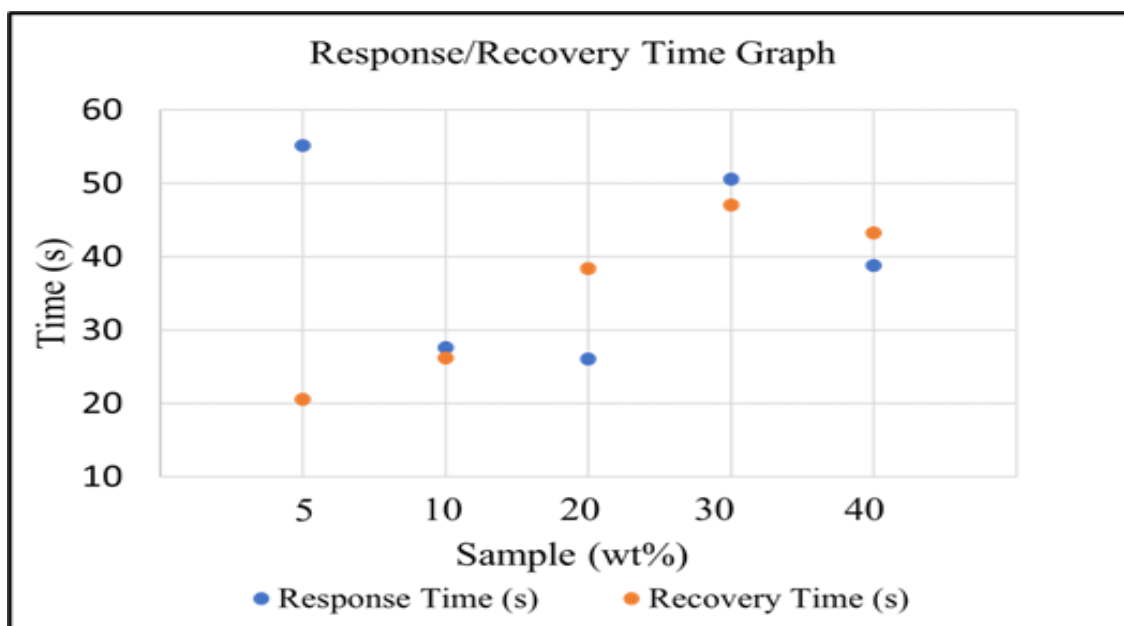


Fig. 7. Comparison of response and recovery time for sample 5wt%, 10wt%, 20wt%, 30wt%, and 40wt% Fe_3O_4 -RGO

The comparison of response/recovery times for samples 5, 10, 20, 30, and 40wt% Fe_3O_4 -RGO are shown in **Fig. 7** and the results were 55.2/20.6, 27.6/26.2, 26.1/38.4, 50.6/47.1, 38.8/43.3s respectively. From the comparison, we can see that the fastest response time was in a sample with 20wt% Fe_3O_4 -RGO and the fastest recovery time was in a sample with 5wt% Fe_3O_4 -RGO. However, the 10wt% Fe_3O_4 -RGO sample had comparable response and recovery times, which makes it ideal compared to the other ratios. This might be due to increasing the analyte site which lead to the increasing of signal detected. For this case, 10wt% is the optimal ratio of the binary hybrid as increasing the ratio beyond this value not improving the response and recovery time of the sensor. This finding proves that tailoring the active material of the MOX sensor can improve the working temperature of the sensor, as well as the response and recovery times.

4. Conclusions

In summary, binary hybrid nanocomposite materials have been synthesized, and a characterization study suggests that the binary hybrid material has a high composition and may blend homogeneously. FTIR analysis revealed that all the peaks from the hybrid nanocomposite matched those of the constituent components. Based on the sensing performance, the response and recovery time of the 10wt% of hybrid Fe_3O_4 -RGO at room temperature was 27.6s and 26.2s respectively. The high operational temperature of the MOX sensor could be reduced to room temperature by hybridizing the active material with RGO, thereby enhancing the response and recovery times. This demonstrates that hybrid material can have a considerable synergistic effect as an active sensing material to increase the sensing capability of the sensor. However, further studies need to be done to investigate the chemical and physical characteristics of the active materials

so that alterations can be made to further lower the response and recovery time as well as improve the sensitivity of the sensor.

Acknowledgement

This research was funded by the Ministry of Higher Education (MOHE) through Fundamental Research Grant Scheme (Ref No. FRGS/1/2019/TK04/UTP/02/7).

References

- [1] C. Arata, P. K. Misztal, Y. Tian, D. M. Lunderberg, K. Kristensen, A. Novoselac, ... & A. H. Goldstein. (2021). Volatile organic compound emissions during HOMEChem. *Indoor Air*. 31 (6), 2099-2117.
- [2] X. Tang, P. K. Misztal, W. W. Nazaroff, & A. H. Goldstein. (2016). Volatile organic compound emissions from humans indoors. *Environmental science & technology*. 50 (23): 12686-12694.
- [3] U. B. Nurmatov, N. Tagiyeva, S. Semple, G. Devereux, & A. Sheikh. (2015). Volatile organic compounds and risk of asthma and allergy: a systematic review. *European Respiratory Review*. 24 (135): 92-101.
- [4] H. Guo, S. C. Lee, L. Y. Chan, & W. M. Li. (2004). Risk assessment of exposure to volatile organic compounds in different indoor environments. *Environmental Research*. 94 (1): 57-66.
- [5] S. C. Sofuoglu, G. Aslan, F. Inal, & A. Sofuoglu. (2011). An assessment of indoor air concentrations and health risks of volatile organic compounds in three primary schools. *International journal of hygiene and environmental health*. 214 (1): 36-46.

- [6] A. Ari, P. E. Ari, S. Yenisooy-Karakaş, & E. O. Gaga. (2020). Source characterization and risk assessment of occupational exposure to volatile organic compounds (VOCs) in a barbecue restaurant. *Building and Environment*. 174: 106791.
- [7] G. Zhang, X. L. Feng, B. Liedberg, & A. Q. Liu. (2016). Gas sensor for volatile organic compounds detection using silicon photonic ring resonator. *Procedia Engineering*. 168: 1771-1774.
- [8] F. A. Tabr, F. Salehiravesh, H. Adelnia, J. N. Gavgani, & M. Mahyari. (2019). High sensitivity ammonia detection using metal nanoparticles decorated on graphene macroporous frameworks/polyaniline hybrid. *Talanta*. 197: 457-464.
- [9] L. Zhu, & W. Zeng. (2017). Room-temperature gas sensing of ZnO-based gas sensor: A review. *Sensors and Actuators A: Physical*. 267: 242-261.
- [10] A. K. Basu, P. S. Chauhan, M. Awasthi, & S. Bhattacharya. (2019). α -Fe₂O₃ loaded rGO nanosheets based fast response/recovery CO gas sensor at room temperature. *Applied Surface Science*. 465: 56-66.
- [11] Z. Cai, & S. Park. (2020). Enhancement mechanisms of ethanol-sensing properties based on Cr₂O₃ nanoparticle-anchored SnO₂ nanowires. *Journal of Materials Research and Technology*. 9 (1): 271-281.
- [12] A. H. N. Athirah, A. B. Chin, W. Y. Hoong, O. B. Hoong, & B. A. Aqilah. (2018). Synthesis and characterization of γ -Fe₂O₃ NPs on silicon substrate for power device application. *Materials Research Express*. 5 (6): 065020.
- [13] M. Gupta, N. Athirah, & H. F. Hawari. (2020). Graphene derivative coated QCM-based gas sensor for volatile organic compound (VOC) detection at room temperature. *Indonesian Journal of Electrical Engineering and Computer Science*. 18 (3): 1279-1286.
- [14] N. A. A. Hussein, H. F. Hawari, & Y. H. Wong. (2021). Synthesis of Iron Oxide/Polyaniline/Reduced Graphene Oxide Nanocomposite Materials as Active Sensing Material. In 2020 8th International Conference on Intelligent and Advanced Systems (ICIAS) (pp. 1-5). IEEE.
- [15] F. Malega, I. P. T. Indrayana, & E. Suharyadi. (2018). Synthesis and characterization of the microstructure and functional group bond of Fe₃O₄ nanoparticles from natural iron sand in Tobelo North Halmahera. *Jurnal Ilmiah Pendidikan Fisika Al-Biruni*. 7 (2): 13-22.
- [16] M. Gupta, H. F. Hawari, P. Kumar, Z. A. Burhanudin, & N. Tansu. (2021). Functionalized reduced graphene oxide thin films for ultrahigh CO₂ gas sensing performance at room temperature. *Nanomaterials*. 11 (3): 623.
- [17] T. Pisarkiewicz, W. Maziarz, A. Małolepszy, L. Stobiński, D. A. Michoń, A. Szkudlarek, ... & A. Rydosz. (2021). Nitrogen dioxide sensing using multilayer structure of reduced graphene oxide and α -Fe₂O₃. *Sensors*. 21 (3): 1011.
- [18] N. A. A. Hussein, H. F. Hawari, Y. H. Wong, & A. S. M. A. Haseeb. (2021). Preparation and sensing characterization of hybrid iron oxide/polyaniline/reduced graphene oxide at room temperature. *International Journal of Chemical and Biochemical Sciences*. 20: 90-95.